Received: 31 March 2016 | Revised: 6 October 2016 | Accepted: 17 October 2016

DOI: 10.1002/gea.21617

RESEARCH ARTICLE

WILEY

# Textural, microstructural, and compositional characteristics of Fe-based geomaterials and Upper Paleolithic ocher in the Lessini Mountains, Northeast Italy: Implications for provenance studies

**Giovanni Cavallo**[1,2] | **Federica Fontana**[3] | **Federica Gonzato**[4] | **Marco Peresani**[3] | **Maria Pia Riccardi**[1] | **Roberto Zorzin**[5]

[1]Department of Earth and Environmental Sciences, University of Pavia, Italy

[2]Institute of Materials and Constructions, University of Applied Sciences and Arts—SUPSI, Campus Trevano, Canobbio, Switzerland

[3]Dipartimento di Studi Umanistici, Sezione di Scienze Preistoriche e Antropologiche, University of Ferrara, Italy

[4]*Soprintendenza* for Archaeological Heritage in Veneto, Operative Unit in Verona, Italy

[5]Civic Museum of Natural History, Lungadige Porta Vittoria, Verona, Italy

**Correspondence**
Giovanni Cavallo, Institute of Materials and Construction, University of Applied Sciences and Arts-SUPSI, Campus Trevano, Canobbio, Switzerland.
Email: giovanni.cavallo@supsi.ch

Scientific editing by Panagiotis Karkanas

## Abstract

Provenance research of archaeological ocher contributes to understanding the capabilities of prehistoric humans to select, process, and treat suitable raw materials for symbolic and utilitarian purposes. The western part of the Lessini Mountains in the Veneto region of northeast Italy is an ideal location for this type of study as it features several different Fe-rich deposits, and many examples of archaeological ocher have been found in the nearby Fumane Cave and Tagliente Rockshelter Upper Paleolithic sites. Sourcing areas are often identified through the use of geochemical studies; however, microscopic techniques can also be used with the benefit of providing more detailed information about accessory minerals and textural characteristics of the material. One of the goals of our study was to demonstrate the potential in using polarizing light microscopy supported by scanning electron microscopy coupled with an energy dispersive X-ray spectrometer in research of this type. We studied geological source samples and archaeological materials from the sites, the results of which are very promising in terms of shedding light on the sourcing of prehistoric ocher in this region.

**KEYWORDS**

archaeological ocher, Fumane Cave, Lessini Mountains, Paleolithic, Tagliente Rockshelter

## 1 | INTRODUCTION

Since the end of the 19th century, natural Fe-rich deposits found in different geological contexts within the western sector of the Lessini Mountains (Venetian Pre-Alps, northeast Italy; Fig. 1) have been identified and characterized (Cavallo, Riccardi, & Zorzin, 2016). Yet, there remains a lack of systematic and detailed research into the geological origins of these deposits. There has traditionally been a consensus among authors on the subject that these geomaterials, characterized by a strong coloring capacity, were used by people as pigments at the local Upper Paleolithic sites of Fumane Cave and Tagliente Rockshelter. This idea—based on the fact that a large quantity of fragments and residues of different sizes were recovered from archaeological layers at both sites—was developed without any scientific evidence except a preliminary investigation on pigment procurement for decorations identified at Fumane Cave (Pallecchi, 2005).

What is known at present about these sites is that (1) archaeological excavations at Fumane Cave have revealed ocher accumulations on the cave floor and painted on stones, and (2) a large quantity of yellow and red ocher fragments found within and in outer areas of Tagliente Rockshelter suggests that such materials were intensively processed at the site, although the purpose of these activities is not yet clear (Fontana et al., 2009). The fragments are found mainly as pieces and sometimes as lumps of ocher, while the powder form is also documented on several stone artifacts and some pebbles (possibly used as pestles and grindstones). Detailed analyses on the archaeological samples and experimental studies have been planned in order to clarify how and why these objects were modified. Massive amounts of chert by-products (Fontana et al., 2009, 2015) also demonstrate that there were intensive processing activities carried out at the site. With the exception of some recent studies (Cavallo, Riccardi, & Zorzin, 2015; Cavallo & Zorzin, 2008, 2014; Gonzato, Castellarin, Chignola, Gamberini, & Lazzeri, 2014), the mineralogical and geochemical characteristics of mineral pigments in the area are poorly known. Likewise, the microstructure, mineralogy, and chemical composition of the ocher recovered from the two archaeological sites

  

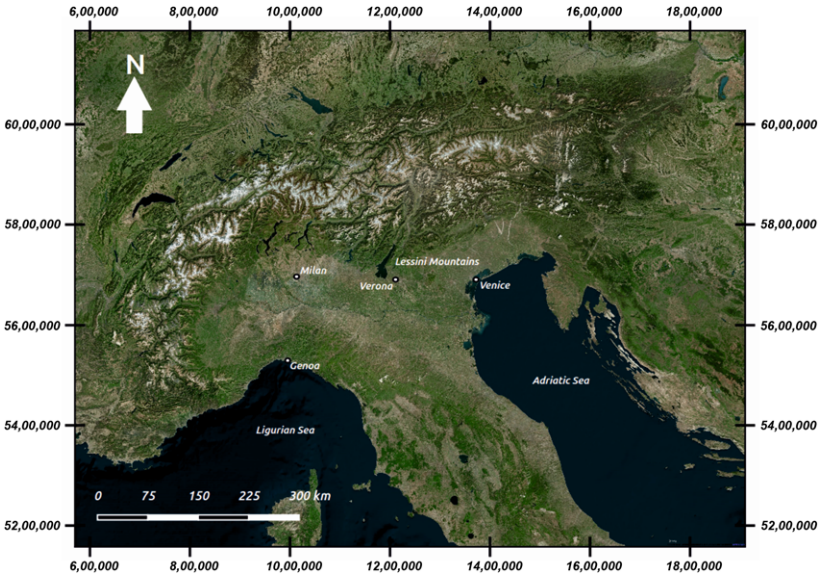


**FIGURE 1** Map of northern Italy and study area located in the western sector of the Lessini Mountains (Map Image Bing Aerial Microsoft Corporation; geographic coordinates: WGS 84 Pseudo Mercator) [Color figure can be viewed at wileyonlinelibrary.com]

during decades of excavations remain poorly defined. This aspect has recently been addressed in an X-ray powder diffraction study at Tagliente Rockshelter (Cavallo, Fontana et al., 2015). Establishing the sources of these coloring materials represents an important part in reconstructing prehistoric hunter-gatherers' interaction with the surrounding environment, including procurement strategies, trade routes used for the transport of natural resources, exchanges with other groups, and the development of social networks (Moreau et al., 2016).

Here, we explore the potential of petrographic examination of geological and archaeological ocher, supported by scanning electron microscopy and X-ray microanalysis, to reveal additional information about these materials and inform provenance studies. Given that coloring Fe-based phases and clay minerals cannot be detected under the optical microscope, information about the texture and microstructure of noncoloring minerals (hereafter "accompanying minerals") can provide diagnostic information when adequate geological survey and sampling are carried out together. The identification of the Fe-based phases requires mineralogical analysis. Moreover, understanding the textural and mineralogical composition of the accompanying minerals is particularly useful in comparing geological and archaeological samples and makes it possible to focus the geochemical investigation of selected archaeological ocher. This is a relatively novel approach to the study of archaeological ochers and is not widely documented with the exception of a few previous studies (Dayet, Texier, Daniel, & Porraz, 2013; Eriarte, Foyo, Sánchez, Tomillo, & Setién, 2009; Pradeau et al., 2016). This type of study augments other scientific approaches to cave and rockshelter research such as geochemical analysis of major and trace elements (Chalmin, Menu, & Vignaud, 2003; Green & Watling, 2007; Macdonald et al., 2011, 2013; Marmolejo-Rodríguez, Prego, Meyer-Willerer, Shumilin, & Sapozhnikov, 2007; Popelka-Filcoff, Robertson, Glascock, & Descantes, 2007; Wadley, 2010), and other quantitative geoarchaeological tests (Woodward & Goldberg, 2001; Woodward, Hamlin, Macklin, Karkanas, & Kotjabopoulou, 2001).

## 2 | GEOLOGICAL SETTING

### 2.1 | Overview of the western Lessini Mountains

Geological features around the city of Verona (Fig. 2) consist of Late Triassic and Miocene formations covered by Quaternary deposits (Zampieri & Zorzin, 1993). Tectonic events associated with the Lessini Mountains influenced the development of karst caves as they formed along a NNE-SSW and NNW-SSE fault system (Zorzin, 1993). These karst systems developed in a subtropical–tropical climate during the late Eocene (*Ponte di Veja*) to the Miocene (*Torricelle*; Zorzin & Stradiotto, 1995).

Associated with the paleokarst phenomena in *Lessinia*, the occurrence of yellow (primarily) and red (secondarily) Fe-based deposits is noteworthy. In this area, paleokarst caves developed within the late Eocene *Priabona* Marls (*Torricelle* mines) during the emergence of the area; the formation outcrops at the top of the hills on the western side of *Valpantena* (valley) and is composed of gray-greenish or gray-yellowish marls rich in *Discocyclinae*. This is the most representative example of the deep karst phenomenon, consisting of over 20 km of dendritic and network galleries, the orientation of which was determined by the tectonic activity in the region.

Earlier paleokarst phenomena also developed during the late Jurassic within *San Vigilio Oolite* and *Rosso Ammonitico Veronese* rock formations (*Ponte di Veja* caves). The *San Vigilio Oolite* (Early-Middle Jurassic) features different stone types such as boundstones, oolites, and encrinites calcarenite, all of which compose the *Ponte di Veja* pillars. The *Rosso Ammonitico Veronese* (Middle-Late Jurassic) is composed of deep red nodular pelagic limestones containing ammonites, belemnites, and stromatolites, and is found in the *Ponte di Veja* large arch.

### 2.2 | Geology of the archaeological sites

The two archaeological sites discussed in this paper are located in the west-central sector of the monoclinal plateau of the Lessini Mountains.

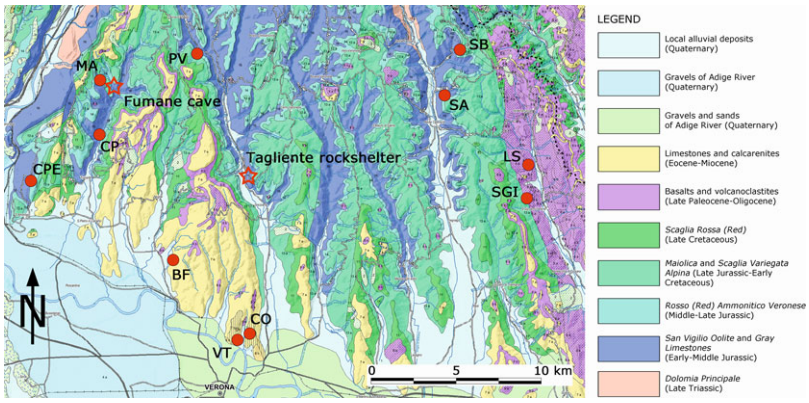


**FIGURE 2** Geological map of the Province of Verona (after A. Zorzin) showing study area and possible sources of ocher (CO, *Colombare* mines; VT, *via Tirapelle* mines; BF, *Buso del Fero* mine; CPE, *Cà de la Pela* mine; CP, *Cà del Paver* outcrop; MA, *Manune* outcrop; PV, *Ponte di Veja* mines; SB, *San Bortolo*; SA, *Sant'Andrea* mine; LS, *Località Salgari* deposit; SGI, *San Giovanni Ilarione* deposits) and archaeological sites (Fumane Cave and Tagliente Rockshelter) [Color figure can be viewed at wileyonlinelibrary.com]

Longitudinal valleys appear as canyons in the northern part and then widen before reaching the alluvial plain of the Adige River (Fig. 2). Tagliente Rockshelter is located at 250 m above sea level (a.s.l.) on the left hydrographic slope of *Valpantena*; Fumane Cave is at 350 m a.s.l. on the left hydrographic slope of *Vajo Roncomerlo*, a small valley near Fumane through which flows Progno Creek.

Mesozoic carbonate formations occur in the area and are locally stratified in large banks with physical discontinuities caused by tectonic activity. Fumane Cave (Fig. 3a) is excavated out of the *San Vigilio Oolite* Formation (Toarcian-Aalenian), that is, locally dolomitized and composed of oolitic limestones rich in echinoderms and crinoids. Tagliente Rockshelter (Fig. 3b) opens at the base of a cliff composed of *Gruppo dei Calcari Grigi* (Hettangian-Pliensbachian). The *Gruppo dei Calcari Grigi* (Group of Gray Limestones) is 450 m thick and is composed of alternating bioclastic and oolitic limestones, gray clayey limestones, and marls.

## 3 | THE ARCHAEOLOGICAL CONTEXTS

### 3.1 | Fumane Cave

Fumane Cave was first explored by the Museum of Natural History of Verona in 1964 and 1982, and has undergone excavation since 1988 by the University of Ferrara (Bartolomei et al., 1992) under the patronage of the Italian Ministry for Cultural Heritage and Tourism. The cave is part of a fossil karst complex whose entrance is completely obstructed by sediment and debris from the collapse of the external part of the roof, which sealed a sheltered area of almost 60 $m^2$ (Fig. 4). It has a 12-m thick sedimentary sequence, divided into four macrounits labeled S, BR, A, and D, which record the main climatic events that occurred between the early and the middle Würm periods (Martini, Sibilia, Croci, & Cremaschi, 2001; Peresani et al., 2008). Macrounit A includes several horizontally layered beds (A13–A1) composed of frost-shattered slabs with variable amounts of sand and eolian dust, the former being prevalent in the western zone (inside the cave) and the latter gradually increasing from the entrance to outside the cave. Stone objects, faunal remains, hearths, and other structures deposited in levels are densely scattered on the ground, particularly in units A11, A10, A9, A6–A5 (Mousterian), and A2, A1 (Protoaurignacian); conversely, less dense groups of these features, isolated combustion structures, and debitage from lithic workshops are preserved in units A5 (final Mousterian), A4, and A3 (Uluzzian). The Late Mousterian and Uluzzian sequences and their cultural remains are described elsewhere (see for instance Fiore et al., 2016; Peresani, 2012; Peresani, Chravzez et al., 2011; Peresani, Cristiani, & Romandini, 2016; Peresani, Fiore, Gala, Romandini, & Tagliacozzo, 2011b; Romandini et al., 2014). Layers A2 and A1 were excavated at different times from 1988 to 2005 in the area of the cave entrance. The archaeological material was either directly excavated using a 33 cm × 33 cm grid, or recovered through wet sieving.

Macrounit D is at the top of the sequence and includes bedrock cavities, outlining the present-day slope morphology. Its formation is mainly due to several rockfalls, followed by stabilization and cryoturbation. Human evidence at the site is recorded in the lower Aurignacian units (D3d, D3b, and D3a), and is more sporadic in the middle Level D1d, in which some Gravettian artifacts were found (Bartolomei et al., 1992). Cultural materials in layer D include bone and antler tools, painted stones, accumulations of ocher, and over 900 mollusk shells (Broglio & Gurioli, 2004; Forte, 2016).

In layer A2, dwelling structures are represented by large hearths, dumps of butchered herbivore carcasses, and stone flaking waste (Broglio & Dalmeri, 2005; Peretto et al., 2004). Layer A2 is discontinuously sandwiched between two large ocher deposits. The smallest deposit is located above A2, at the cave entrance (structure 21), and the largest unit (A2R) extends to the rear of the cave (Fig. 4). In addition, sediment from A2 has produced numerous examples of small fragments of red and yellow ocher and many red stained stones have been found in layers A2–D3.

A revised chronology of the middle–late Paleolithic sequence (Douka et al., 2014; Higham et al., 2009) has shown that the beginning and the end of Level A2 date, respectively, to 41,900–40,200 cal. yr B.P. and 40,300–39,400 cal. yr B.P. at the largest confidence interval (Douka et al., 2014; Higham et al., 2009).

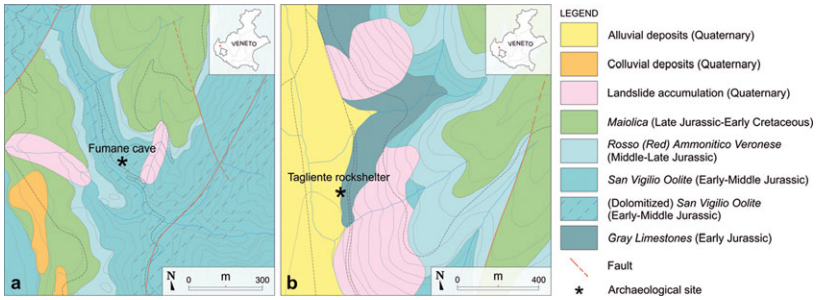


**FIGURE 3** Detailed geological maps of the area around Fumane Cave (a) and Tagliente Rockshelter (b); maps based on Municipal geological cartography (elaboration by S. Zannotti) [Color figure can be viewed at wileyonlinelibrary.com]

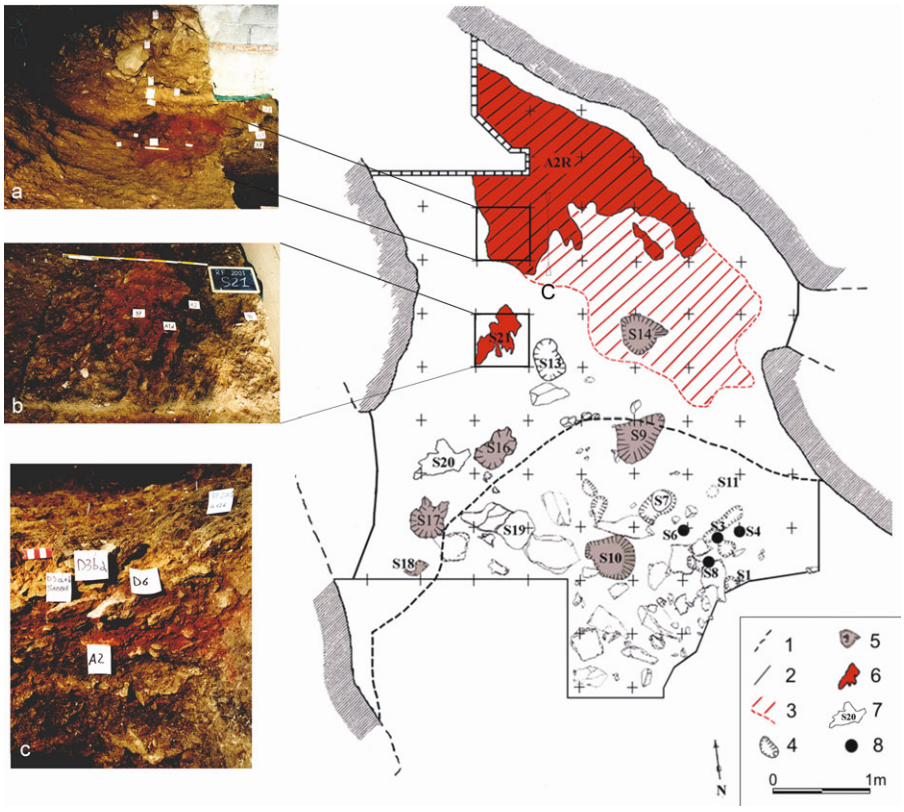


**FIGURE 4** Fumane Cave; plan of the cave showing the structures and the distribution of ocher in the oldest Aurignacian stratigraphic complex (unit A2 and related); key: 1, present-day entrance of the cave; 2, perimeter of the excavation; 3, sediment with sparse ocher; 4, shallow basin of anthropic origin; 5, fireplace; 6, large ocher deposits (structure 21 and A2R); 7, dump; 8, postholes (modified by Broglio & Dalmeri, 2005; Peretto et al., 2004); images on the left: (a) view from the south of the largest concentration of ocher (layer A2R) exposed at the base of the macrounit D; (b) structure 21 exposed at the top of layer A2; (c) section showing the layer A2R sandwiched between layers A2 and D6. The position of the section is indicated on the map [Color figure can be viewed at wileyonlinelibrary.com]

## 3.2 | Tagliente Rockshelter

The site of Tagliente (Fig. 5) lies under a wide rockshelter at the base of *Monte Tregnago*. From 1962 until 1967, the site was excavated by the Museum of Natural History of Verona, and then from 1967 to the present by the University of Ferrara. Its complete stratigraphic sequence is about 4.60 m thick and has been divided into two main units separated by an erosion surface of alluvial origin. The lower unit is attributed to the early and middle Würm periods and contains Mousterian and Aurignacian lithic industries, while the upper unit dates to the late Würm period and is culturally related to the late Epigravettian period (Arzarello & Peretto 2005; Bartolomei et al., 1982, 1984; Bertola et al., 2007; Fontana et al., 2009; Thun Hohenstein & Peretto, 2005). Only the upper unit has yielded a considerable amount of ocher fragments that are the subject of this paper.

Taking into account the available radiocarbon dates, which range from 17,100–16,300 cal. yr B.P. (layer 13a$\alpha$) to 14,570–13,430 cal. yr B.P. (Levels 10–8), the Epigravettian occupation spans from the final phase of the Ancient Dryas to the first part of the Bølling–Allerød interstadial (Fontana et al., 2009, 2012, 2015).

Extensive archaeological investigations have been carried out in the last three decades in the northern part of the site, over an area of about 80 m$^2$ within the Epigravettian series. These excavations have shown

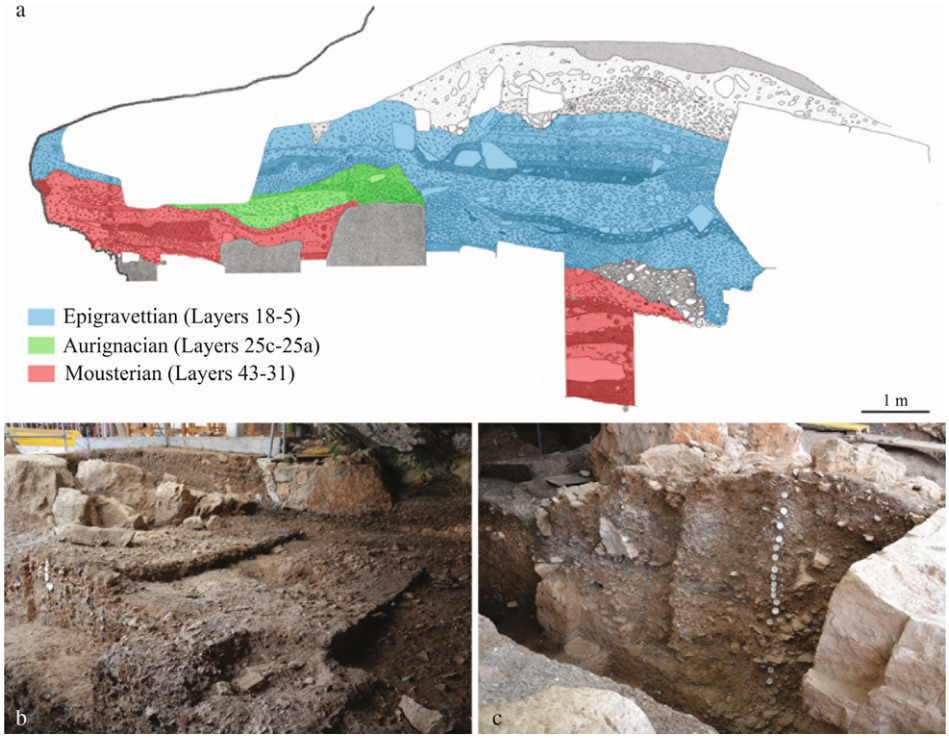


**FIGURE 5** Tagliente Rockshelter; (a) stratigraphic sequence of the transverse trench; (b) view of the late Epigravettian deposits from the interior of the shelter; (c) detail of the late Epigravettian stratigraphic sequence of the transverse trench in the external area of the site (photographs by D. Visentin) [Color figure can be viewed at wileyonlinelibrary.com]

the presence of a recurrent pattern in the organization of living areas (Bartolomei et al., 1984; Bertola et al., 2007; Fontana et al., 2008, 2009, 2015; Fontana, Guerreschi, & Liagre, 2002; Guerreschi, 1983; Peretto et al., 2004) that are characterized by (1) an inner area where only the lower Epigravettian layers are preserved and that present thick habitation soils and some dwelling structures, for example, a series of fireplaces around which different domestic and processing activities took place, and (2) an outer area where there is a significant concentration of various materials connected with human activity, such as lithic waste products and animal bone remains (Cilli & Guerreschi, 2000; Cremona & Fontana, 2007; Fontana et al., 2008, 2009; Rocci Ris, Cilli, Malerba, Giacobini, & Guerreschi, 2005).

All Epigravettian layers document intense knapping activity and exploitation of the locally abundant supply of chert (Arzarello et al., 2007; Bertola et al., 2007; Bietti et al., 2004; Fontana et al., 2015). Tagliente Rockshelter has also yielded one of the most important collections of tools and ornamental objects made of animal hard tissues, and the richest assemblage of marine shells, both perforated and unmodified, of the whole Italian Late Epigravettian period, composed of more than 1000 specimens (Cilli, Giacobini, Guerreschi, & Gurioli, 2006).

A significant quantity of ocher nodules and fragments has been collected both in the inner and outer areas of the site, amounting to more than 8 kg from all the stratigraphic units explored. Although there is no specific association with the fireplaces, the nodules and fragments (especially the red types) appear in greater numbers in the inner area (Fontana et al., 2009). Of great importance is also a group of small-scale art objects with incision marks. Only a few items are either associated with, or show the presence of, ocher traces, the study of which is still in progress (Guerreschi & Veronese, 2002). A partial burial, assigned a radiocarbon date of 16,630–15,290 cal. yr B.P., was discovered in the 1970s in the southern part of the site, and included among other objects, a limestone pebble with some traces of ocher (Bartolomei et al., 1974, 1984; Gazzoni et al., 2013).

## 4 | MATERIALS AND METHODS

### 4.1 | Yellow and red natural Fe-based raw materials (potential geological sources)

The yellow and red Fe-based deposits in the area are associated with Mesozoic and Tertiary carbonate formations; just one outcrop is associated with volcanic rocks (Eocene basalts). In most of the studied sites, the natural Fe materials are in the form of laminar deposits of variable thickness, composition, and color filling the palaeokarst caves. Massive yellow Fe-based deposits were found in two cases as infilling sediments of palaeokarst caves, and significant yellow and red Fe-based deposits lie in stratigraphic continuity with basalts. The location and the description of the most representative yellow and red geomaterials collected within a radius of approximately 20 km from the archaeological sites are listed in Table I; sampling areas and archaeological sites are reported in Figure 2.

Direct observation of the Fe-based deposits inside the caves was possible exclusively on the lateral walls of the galleries where some remnants still exist even after the intense mining during the last

**TABLE I** Location and description of the natural Fe-based geomaterials

| | Location of Host and Parent Rocks | Description |
|---|---|---|
| SA | *Sant'Andrea* Cave is associated with Mesozoic *Complesso Dolomitico Indifferenziato* (Undifferentiated dolomitized complex). (Val d'Illasi; locality: *Sant'Andrea*). | The observed yellow deposit is massive and quite homogeneous except for a pocket where red material was collected. Samples ($n = 4$) were taken along a vertical profile ~1.5 m high from the lateral wall. |
| CPE | *Cà de la Pela* palaeokarst cave is associated with Mesozoic dolomitized oolitic limestones (municipality: S. Ambrogio di Valpolicella; locality: *Ca' de la Pela*). | The deposit is layered exhibiting a folded morphology. The individual layers are rather homogeneous exhibiting color ranging from yellow to brown. Samples ($n = 4$) corresponding to the two colors were collected from the sequence that covers the front wall at the end of the cave. The entire sequence is ~2 m high. |
| SB | *San Bortolo* outcrop is associated with Mesozoic *Complesso Dolomitico Indifferenziato* (undifferentiated Dolomitized Complex). (Selva di Progno: locality: *San Bortolo delle Montagne*). | The deposit outcrops out along an artificial trench opened in the past for the construction of the road. The profile has a variable thickness (0.5–2.0 m) and the carbonate host rock is markedly folded. Yellow-brown ocher occurs as infilling material; samples ($n = 4$) were collected along the vertical profile. |
| MA | *Manune* outcrop is associated with Mesozoic Dolomitized oolitic limestones (Fumane; locality: *Manune*). | Three small outcrops were considered (two red and one yellowish) close to Fumane Cave, along the road which goes to Manune village. One sample was collected from each outcrop. |
| PV | *Ponte di Veja* palaeokarst system develops at the contact between the Mesozoic oolitic limestones and the Rosso Ammonitico Veronese Formations (Sant'Anna d'Alfaedo). | Samples were collected at Caves A, D = E, and G. Samples from Cave A ($n = 5$) were collected from the left wall with respect to the entrance where the thickness of the deposits is approximately 1 m; the deposit is rather homogeneous even if thin laminae can be recognized; fragments of carbonate rocks are distinguishable. Samples in the Cave D = E ($n = 3$) were collected from the left wall (with respect to the entrance) where the sequence is approximately 1 m high; alternating layers of dark brown and lighter colored material can be seen, cementing blocks of carbonate rocks fallen down from the vault of the cave. Samples from the Cave G ($n = 3$) were collected from the front. |
| CP | *Cà del Paver* outcrop is associated with Mesozoic dolomitized gray limestones (Fumane; locality: *Ca' del Paver*). | Samples ($n = 2$) were collected from an outcrop visible along the road which goes to Fumane at *Cà del Paver* locality. The samples consist of pale yellow fragments of dolomitized limestone. |
| VT | Via Tirapelle palaeokarst system is associated with Eocene limestones (Verona; locality: *Valdonega*). | Samples were taken from laminar deposits filling the palaeokarst network. Samples named VTf ($n = 8$) were taken from the layered deposit at the end of the principal corridor; samples TP ($n = 5$) from the principal corridor; samples VT-S ($n = 6$) from the layered sequence at the end of the branch called *squalo*, shark). VTf, TP, and VT-S samples correspond to individual layers of the collected layered sequence. |
| CO | Colombare palaeokarst system is associated with Eocene limestones (Verona; locality: *Valdonega*). | Samples were collected from the stations A ($n = 7$), B ($n = 3$), and C ($n = 3$) moving from the base of the artificial shaft 18 m deep. |
| BF | *Buso del Fero* mine is at the contact between the Eocene volcanoclastic terrain and the Eocene limestones (Negrar municipality). | Samples were collected from different galleries—A (3): main gallery, B (2) and C (3): upper levels of the main gallery. |
| SGI | Eocene basalts (San Giovanni Ilarione; locality: Viale). | Samples ($n = 2$) were collected from the main outcrop that is located on private land and from the sequence close to the previous one where yellow earth ($n = 1$) is associated with red earth ($n = 1$). |
| LS | Eocene basalts (San Giovanni Ilarione; locality: Salgari). | Samples ($n = 2$) were collected from a limited outcrop that is located on private land. |

century. In several cases, sampling was problematic due to the existence of narrow passages, perilous safety conditions, the presence of standing water, and the fact that the deposits are located on private property. However, despite these difficulties, the collected samples are representative of the geological environment and the whole stratigraphic sequence.

In terms of the origin of these sediments, information is limited as no detailed studies have yet been conducted, and because existing studies focused only on the hills around Verona. According to the most recent of these studies (Gonzato et al., 2014), the yellow Fe-based materials deposited in paleokarst caves are a consequence of erosional processes that affected lateritic paleosols that developed on Eocene volcanic rocks. However, this interpretation requires more in-depth study as it is based just on the Al and Fe content of five samples investigated in a previous work (Cavallo & Zorzin, 2008) concerning deposits in the Eocene limestones around Verona.

## 4.2 | Ocher from archaeological sources: Fumane cave and Tagliente rockshelter

Samples from Fumane Cave were taken from Aurignacian Levels A and D and are described in Table II, including modifications of the artifacts noted by Hodgskiss (2010) and Rifkin (2012). Approximately 120 red and yellow ocher samples were collected from the interior and exterior parts of Tagliente Rockshelter from all excavated stratigraphic units both in vertical (diachronic) and horizontal (synchronic) directions. In the current study, additional samples were collected based on characteristic mineral assemblage groupings (Cavallo, Fontana et al., 2015). Sample descriptions are reported in Table III. For both archaeological ocher sets, Munsell color notation refers to the bulk color of the fragment excluding postdepositional material prior to mechanical grinding for X-ray powder diffraction and to the powder.

All the analyzed archaeological ocher fragments were initially observed under binocular microscope. Both raw geomaterials and

**TABLE II** Fumane cave ocher samples

| | | | Munsell Color | | Description | | |
|---|---|---|---|---|---|---|---|
| Macrounit | Context | Square | Massive | Powder | Morphology, Structure, and Superficial Characteristics | Wear Traces | |
| A | A1 | 72g | 2.5 Y 7/8 | 2.5 Y 7/8 | Rounded homogeneous fragment; cohesive (lump of ocher) | | U-shaped erratically oriented grooves |
| | A1 | 72b | 10 R 4/8 | 10 R 5/8 | Subrounded fragment almost homogeneously coated with a red ferruginous patina; cohesive (fragmented piece) | No | |
| | A1 | 72h | 10 R 4/8 | 10 R 4/8 | Subrounded/subangular fragment almost homogeneously coated with a red ferruginous patina; cohesive (fragmented piece) | No | |
| | A2 | 90e | 10 YR 7/8 | 5 YR 5/8 | Well-rounded sample showing color gradually turning from yellow to red (heating treatment?); cohesive (lump of ocher) | No | |
| | A2 | 96-97 | 10 R 4/8 | 10 R 5/8 | Subangular fragment almost homogeneously coated with a red ferruginous patina; cohesive (fragmented piece) | No | |
| | A2 | 77c | 10 YR 6/8 | 7.5 YR 6/6 | Subangular sample showing black spots (contact with embers?); cohesive (lump of ocher) | No | |
| | A2 | 46g | 10 R 3/6 | 2.5 YR 4/8 | Subangular fragment almost homogeneously covered with a red ferruginous patina; cohesive (fragmented piece) | No | |
| | A2 | 110d | 10 R 6/6 | 5YR 8/4 | Angular flake of limestone partially coated with a thin pinkish patina; cohesive (fragmented piece) | No | |
| | A1 + A2 | 97 | 10 R 4/4 | 10 R 5/4 | Subrounded fragment almost homogeneously coated with a red ferruginous patina; cohesive (fragmented piece) | No | |
| | A2R | 126g(1) | 10 R 4/6 | 2.5 YR 5/6 | Subrounded fragment almost homogeneously coated with a red ferruginous patina; cohesive (fragmented piece) | No | |
| | A2R | 126g(2) | 10 R 6/6 | 5YR 7/6 | Angular flake of limestone partially coated with a pinkish patina; cohesive (fragmented piece) | No | |
| | A2R | 147h | 10 R 3/4 | 10 R 4/6 | Subangular homogeneous fragment showing traces black in color (contact with embers?); cohesive (fragmented piece) | | Metallic luster |
| | A2R | 147h | 10 YR 5/8 | 10 YR 6/8 | Subangular homogeneous fragment showing traces black in color (contact with embers); cohesive (fragmented piece), convex surface | No | |
| D | D3 | 137d | 10 YR 6/6 | 10 YR 7/8 | Subrounded homogeneous fragment showing traces black in color (contact with embers?); cohesive (lump of ocher), convex surface | | U-shaped erratically oriented grooves |
| | D3 | 137d | 10 R 4/4 | 10 R 4/8 | Subrounded homogeneous fragment; cohesive (fragmented piece) | No | |
| | D6 | 125c | 10 R 3/6 | 2.5 YR 4/8 | Rounded carbonate rock fragment partially coated with a red ferruginous patina; cohesive (fragmented piece) | No | |
| | D3d | 68a | 10 R 4/6 | 10 R 5/8 | Angular carbonate rock fragment partially coated with a red ferruginous patina; cohesive (fragmented piece) | No | |
| | D3d | 68b | 10 R 6/3 | 10 R 5/6 | Angular carbonate rock fragment partially coated with a red ferruginous patina; cohesive (fragmented piece) | No | |

**TABLE III** Tagliente Rockshelter ocher samples: interior (a) and exterior series (b)

| Macrounit | Context | Square | Munsell Color Notation | | Description | Wear Traces | |
|---|---|---|---|---|---|---|---|
| | | | Massive | Powder | Morphology, Structure, and Superficial Characteristics | | |
| **(a)** | | | | | | | |
| 1st | 302 | 55/8 | 10 R 3/6 | 10 R 4/8 | Subangular fragment with an off of white patina on the surface. The interior exhibits well-preserved microlaminations disposed along parallel beds; cohesive (fragmented piece) | No | |
| 2nd | 359 | 69/2 | 10 YR 6/6 | 10 YR 6/8 | Subangular fragment with a dark patina on the surface; cohesive (fragmented piece) | No | |
| 3rd | 358 | 69/3 | 10 R 5/8 | 10 R 5/8 | Subangular, coherent fragment. Probable presence of carbonates of secondary origin; cohesive (fragmented piece) | No | |
| | 13A$\alpha$ | 85/6 | 10 R 3/6 | 10 R 4/8 | Subangular fragment with a dark patina on the surface. Microlaminations and bright crystals are visible along the transversal section; cohesive (fragmented piece) | No | |
| | 13 | 39/2 | 10 R 4/6 | 10 R 5/8 | Subangular fragment with an off of white patina on the surface and, locally, accumulation of a secondary sandy-silty deposit; cohesive (fragmented piece) | | U-shaped erratically oriented grooves |
| | 13$\alpha$ | 42/3 | 10 R 3/6 | 10 R 4/6 | Subrounded sample with a dark patina on the surface; cohesive (fragmented piece) | No | |
| | 13 | 69/6 | 10 R 4/6 | 10 R 4/8 | Subangular fragment with a dark patina on the surface; cohesive (lump of ocher) | No | |
| T12 | 12 | 54/1,2,3 | 10 R 4/6 | 2.5 YR 6/4 | Subangular, coherent, and massive fragment with an off of white patina and some black areas on the surface; the inner color is gray (5 Y 5/1) corresponding to a stone; cohesive (fragmented piece) | | U-shaped crossed grooves |
| **(b)** | | | | | | | |
| T4 | 4(b) | 22 | 2.5 YR 2.5/4 | 10 YR 4/8 | Subangular fragment with an off of white patina and some black areas on the surface. Microlaminations are slightly evident on the fresh-cut transversal section; cohesive (fragmented piece) | No | |
| T5 | 5 | 22 | 10 YR 5/8 | 10 YR 6/8 | Subangular fragment with a dark patina on the surface; cohesive (fragmented piece) | No | |
| T6 | 6 | 6 | 10 YR 5/8 | 10 YR 5/8 | Subrounded sample with a dark patina; traces of orange ocher powder are visible; cohesive (fragmented piece) | No | |
| | 6 | 6 | 10 R 3/6 | 10 R 4/6 | Subrounded sample with dark spots and gray deposits irregularly distributed over the surface. Microlaminations and microcracks are visible; cohesive (fragmented piece) | No | |
| T7 | 7 | 80/7 | 10 YR 5/6 | 10 YR 7/8 | Angular and layered fragment with brown microlaminations disposed horizontally along parallel beds; it exhibits visible bright crystals; cohesive (fragmented piece) | No | |
| T8 | 8 | 20/2 | 10 YR 5/6 | 7.5 YR 5/8 | Subrounded sample exhibiting visible microlaminations on the external surface; cohesive (fragmented piece) | No | |
| | 8 | 51/6 | 10 R 3/3 | 2.5 YR 4/8 | Subangular and massive fragment coated with a dark patina; cohesive (fragmented piece) | No | |

(continues)

**TABLE III** *(Continued)*

| (a) | | | | | | | |
|---|---|---|---|---|---|---|---|
| | | | Munsell Color Notation | | Description | | |
| Macrounit | Context | Square | Massive | Powder | Morphology, Structure, and Superficial Characteristics | Wear Traces | |
| T9 | 9 | 23 | 10 YR 5/6 | 10 YR 6/8 | Subrounded sample exhibiting brown microlaminations disposed horizontally along parallel beds; cohesive (fragmented piece) | No | |
| T10 | 10a | 80/4 | 10 R 3/6 | 10 R 4/8 | Subangular fragment coated with a dark silty patina; cohesive (fragmented piece) | No | |
| | 10a | 80/4 | 10 YR 5/6 | 10 YR 5/8 | Subrounded sample exhibiting microlaminations along the transversal fresh-cut surface; cohesive (fragmented piece) | No | |
| | 10b | 80/7 | 10 YR 5/6 | 10 YR 5/8 | Subrounded sample exhibiting black areas on the surface; cohesive (fragmented piece) | No | |
| | 10c | 8 | 10 YR 5/6 | 10 YR 6/8 | Subrounded sample exhibiting microlaminations along the transversal fresh-cut surface; cohesive (fragmented piece) | No | |
| | 10d | 64/8 | 10 YR 6/8 | 7.5 YR 5/8 | Subangular fragment coated with a whitish-grayish patina; cohesive (fragmented piece) | No | |
| | 10f | 37 | 10 R 3/6 | 10 R 3/6 | Subrounded sample with a silty-sandy patina irregularly distributed on the surface; cohesive (fragmented piece) | No | |
| T11 | 11A | 35/8–34/2 | 10 R 2.5/2 | 5 YR 3/3 | Well-rounded sample; cohesive (fragmented piece) | | U-shaped crossed grooves |
| | 361 | 53/1 | 10 R 4/8 | 10 R 4/8 | Subangular, homogeneous fragment with cracks, and microcracks on the external surface; cohesive (fragmented piece) | No | |
| T12 | 363 | 82/6(Ya) | 10 YR 5/8 | 10 YR 6/8 | Subangular, homogeneous fragment with white spots distributed irregularly over the surface; cohesive (fragmented piece) | No | |
| | 363 | 82/6(Yb) | 10 YR 5/8 | 10 YR 6/8 | Subrounded, homogeneous sample; cohesive (fragmented piece) | No | |
| | 12 | 8 | 10 R 3/6 | 10 R 4/8 | Angular, homogeneous fragment almost totally coated with a thick gray patina; cohesive (fragmented piece) | No | |
| | 12 | 25 | 10 YR 5/6 | 10 YR 6/8 | Subangular and massive fragment with an off of white patina and black spots spread around; cohesive (fragmented piece) | No | |
| T13 | 13 | 8 | 10 R 3/6 | 10 R 4/8 | Subrounded, homogenous sample covered with a thick sandy-silty patina; cracks are visible on the surface; cohesive (lump of ocher) | No | |
| T13–T14 | 365 | 79/2 | 10 YR 5/8 | 7.5 YR 5/8 | Angular, quite homogeneous fragment (1.0–1.5 mm ø pink inclusion) covered with a silty-sandy deposit; black spots are scattered over the surface; cohesive (fragmented piece) | No | |
| | 418 | 50/1 | 10 YR 5/8 | 10 YR 6/8 | Subrounded sample with a patina over the surface and signs of microlaminations; cohesive (fragmented piece) | No | |
| T15 | 15 | 22 | 10 R 4/6 | 10 R 5/8 | Well-rounded sample; cohesive (lump of ocher) | No | |
| T16 | 16 | 22 | 10 R 3/6 | 10 R 4/6 | Angular fragment with a dark well-cemented thick patina irregularly distributed over the surface | No | |

archaeological ocher were then examined under a polarizing light microscope (PLM). Thin sections of the archaeological ocher were left uncovered in order to eventually allow them to be studied using other analytical techniques such as scanning electron microscopy/energy-dispersive X-ray spectrometry (SEM/EDXS). Samples were impregnated with epoxy resin to prevent disintegration during sectioning. A Zeiss Axioskop 4.0 PLM was used, and images were captured with a digital camera and processed with the software Axiovision (Zeiss, release 4.5.1).

As a complementary tool, representative samples were analyzed under a Field Emission Gun (FEG) SEM/EDXS; a Tescan Mira 3XMU-series FE-SEM equipped with an EDXS was used. The instrumental setup was as follows: accelerating voltage, 20 kV; HV, beam intensity 16.5; absorbing current 2.1 pA; counts of 100 s/analysis; and working distance 15.8 mm.

## 5 | RESULTS

### 5.1 | Raw geomaterials

The coloring mineral phase of all the studied raw geomaterials is goethite (yellow samples) and hematite (red samples) as reported in Cavallo, Riccardi et al. (2015). Descriptions are reported in Table I.

#### 5.1.1 | Raw geomaterials associated with Mesozoic dolomitized limestones

Yellow-brown and red geomaterials are associated with *Complesso Dolomitico Indifferenziato* (SA, SB), dolomitized oolitic limestones (CPE, MA), and *Calcari Grigi Dolomitizzati* (dolomitized gray limestones; CP), generally indicated as Mesozoic dolomitized limestones. These occur as consolidated deposits filling karst fractures (SA, SB); in a few cases (CP, MA) they occur as outcrops of limited extension. The prevailing colors (SA, SB, CP) are yellow and brown and are due to the presence of goethite; using the present experimental XRD setup, which cannot avoid contaminating Fe-K$\alpha$ fluorescence (Cavallo, Fontana et al., 2015), this mineral was not detected in the samples from CP, its weight percentage likely falling below the few percent level. Additionally, SA paleokarst cave deposits show limited hematite-rich red pockets, while the red color in the MA outcrops, for the reason outlined above, could not be assigned to any detectable amount of hematite.

All the collected samples are homogeneous and rather coherent. Although the mineralogical composition slightly differs from one site to another, petrographic examination enabled a clear distinction based on textural and microstructural characteristics. In the samples from *Sant'Andrea* Cave (SA), it is possible to state that goethite—and hematite in a limited pocket—accompanying minerals is represented primarily by euhedral ferroan dolomite with diameters of 50–100 $\mu$m, and secondarily by calcite. In some instances, ferroan dolomite is subhedral with ferruginous inter- and intracrystalline alteration; veins filled with secondary calcite occur at this site as well.

The distribution of goethite and ferroan dolomite in the samples from *San Bortolo* (SB) is along markedly folded microlaminations indicating postdepositional deformation induced by tectonic activity. Ferroan dolomite crystals are euhedral and zoned, the size is generally 100 $\mu$m across; the maximum crystal size is 300 $\mu$m across. In addition, dolomite appears as anhedral crystals showing an intense ferruginization along the intercrystalline contacts. The crystal diameter generally ranges between 25–50 and 100 $\mu$m.

Samples from *Ca' del Paver* (CP) exhibit a mosaic of anhedral dolomite crystals with predominant crystal diameters of 25–50 $\mu$m and ferruginous weathering along the intercrystalline contacts.

Samples from *Manune* (MA) exhibit euhedral zoned ankerite crystals having a nucleus rich in Fe-oxides; sometimes ankerite crystals are anhedral and surrounded by Fe-oxides; secondary calcite occurs as well. Crystal diameters range between 20 and 300 $\mu$m. The deformation of crystals in these samples is quite evident.

Materials from *Cà de la Pela* (CPE) occur as infill deposits of a paleokarst cave. They appear as laminar and wavy alternating yellow and brown layers with variable thicknesses ranging from a few millimeters to a few centimeters. The brown layers show white microlaminae due to carbonates. The coloring mineral phase is goethite; accompanying minerals are euhedral–subhedral crystals of carbonates with edges exhibiting alteration due to the presence of Fe-oxide. The use of X-ray Powder Diffraction XRPD allowed for the identification of the carbonates as ankerite (Cavallo, Riccardi et al., 2015). Sometimes pseudomorphs of goethite after dolomite were noted. Crystal diameter ranges between 50 and 200 $\mu$m. Ankerite crystals are disposed along microfolds due to plastic deformations of the sediments; microfaults due to fragile deformations also occur.

#### 5.1.2 | Raw geomaterials associated with Mesozoic limestones

Yellow Fe-based geomaterials associated with *Oolite di San Vigilio* (*San Vigilio* Oolite) *and Rosso Ammonitico Veronese* (*Veronese* Red Ammonitic Limestones) occur *at Ponte di Veja* (PV). Representative samples collected in the three palaeokarst caves (Caves A, G, and D = E) belong to two main groups: laminar deposits that are most common, and nonlaminar Fe-based material found mainly associated with brecciated fronts as is clearly visible in Cave G.

A characteristic laminar sample consists of the following sequence: (1) a 3-mm thick layer composed of goethite and calcite crystals 50–100 $\mu$m across, (2) a 2-mm thick layer composed of goethite and 0.5–1.0 mm fragments of oolitic limestone, ooids, and rare fragments of bioclasts (echinoderms), (3) a 4-mm thick layer featuring intermediary characteristics of the previous two layers, (4) a 0.2-mm thick layer composed of goethite without any clastic fraction, and (f) a 2-mm thick layer exhibiting the same characteristics as layer i.

Other samples are composed of quartz and goethite. Under PLM, Fe-oxyhydroxides show a homogeneous distribution and microlaminar sequences. Detailed observation under the electron microscope allowed for the identification of biomineralization processes developed by Fe oxidizing bacteria (Fig. 6a–d; Konhauser, 2016, personal communication).

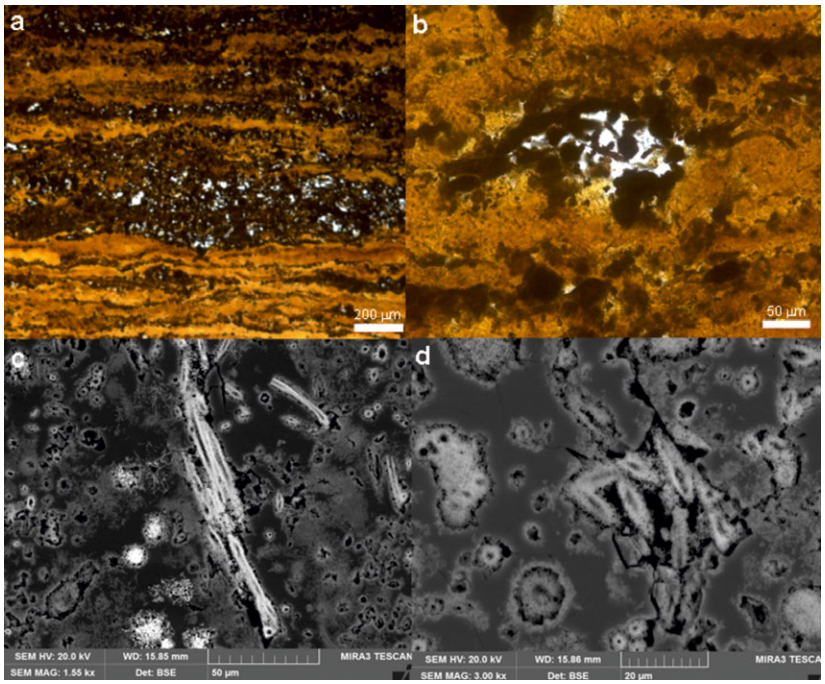


**FIGURE 6** *Ponte di Veja* potential sourcing area, Cave G; (a) quartz-rich goethite exhibiting characteristic microlaminations (PLM, PPL, image width = 1.8 mm); (b) subrounded and elongated goethite crystal morphologies (PLM, PPL, image width = 0.45 mm); (c and d) elongated and subrounded morphologies of goethite crystals revealing the biomineralization process affecting the original quartz due to Fe-oxidizing bacteria (BSE pictures) [Color figure can be viewed at wileyonlinelibrary.com]

### 5.1.3 | Raw geomaterials associated with Eocene limestones

Yellow Fe-based geomaterials are associated with Eocene limestones at *Via Tirapelle* (VT) and *Colombare* paleokarst caves (CO). The deposits fill paleokarst caves and exhibit microlaminar microstructure at the macroscale due to the alternation of goethite- and carbonate-rich laminae. Two representative samples were selected for each cave characteristic of the Eocene limestone paleokarst systems (Fig. 7a–f). The sequence consists of several layers with layer 1 subdivided into four sublayers: (1a) a 0.7-mm thick layer composed of a silico-clastic skeleton (subangular quartz crystals about 50 $\mu$m in diameter, euhedral and subhedral dolomite crystals 25 $\mu$m in diameter, glauconitic minerals sometimes altered into Fe-oxides, plagioclases, muscovite, and subordinately biotite), (1b) a 0.4-mm thick layer similar to 1a but with a greater amount of goethite and a markedly lower amount of glauconitic minerals; (1c) a 0.2-mm thick layer composed of carbonates and quartz; and (1d) a 1.0-mm thick layer composed of Fe-oxides associated with minor amounts of quartz, dolomite, and muscovite. The remaining sequence consists of (2) a 2.3-mm thick layer composed of Fe-oxides and subangular quartz crystals 50 $\mu$m across, muscovite, dolomite/ferroan dolomite, and glauconitic minerals; (3) a homogeneous layer composed of Fe-oxides associated with dolomite crystals and rarely quartz and muscovite; (4) similar to layer 2; and (5) similar to layer 3.

The red sample from the "shark" gallery of the *via Tirapelle* mine features several layers. Layer 1 is a layer rich in glauconitic minerals both altered and unaltered, sometimes with inclusions of euhedral crystals of dolomite; glauconitic minerals are well-rounded, with a grain size

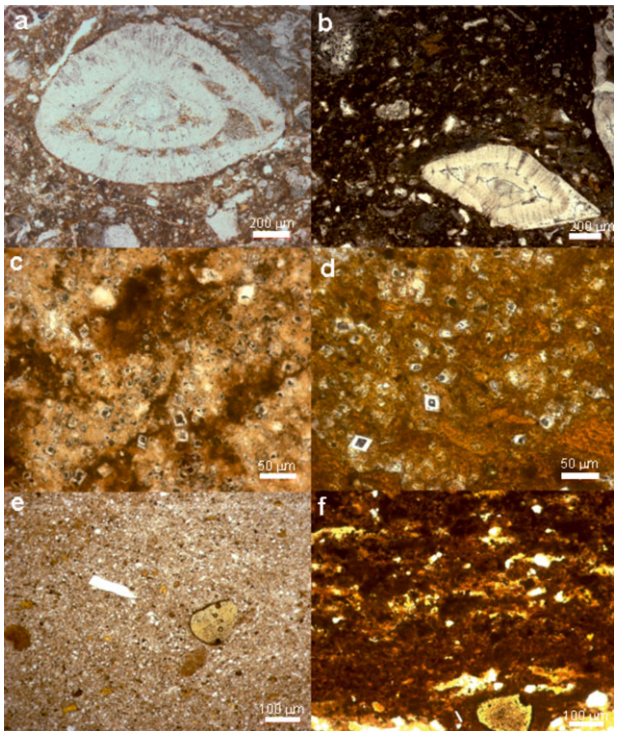


**FIGURE 7** *Colombare* (images a, c, e) and *via Tirapelle* (images b, d, f) paleokarst caves: Fe-based geomaterials occurrences; (a and b) large *Nummulites* sp. (benthic *Foraminifera* characteristic of the Middle Eocene), size 0.6–0.8 mm across; (c and d) euhedral zoned dolomite crystals 25 $\mu$m across; (e and f) glauconitic minerals (all micrographs under PLM, PPL; a and b images width = 1.8 mm; c and d images width = 0.45 mm; e and f images width = 0.9 mm) [Color figure can be viewed at wileyonlinelibrary.com]

ranging 0.3–0.4 mm. Also present are subangular quartz grains 30–40 $\mu$m in diameter and exceptionally subrounded grains 200 $\mu$m in diameter with wavy extinction and other accompanying minerals such as calcite and euhedral dolomite, muscovite, chloritized biotite, chert, and altered feldspars. The matrix is red and composed of hematite. Layer 2 exhibits textural characteristics that are different from layer 1, but the mineralogical composition is the same; the most important differences are found in grain size distribution, the drastic reduction of the glauconitic minerals, and a major amount of dolomite crystals. Quartz and carbonates measuring 50 $\mu$m in diameter are the prevailing mineral phases; muscovite is secondary and glauconitic minerals and altered biotite are accessory phases. Layer 3 demonstrates many microlaminae due to the content of coloring (hematite) and noncoloring (dolomite) components. Other samples exhibit characteristic bioclasts such as *Nummulites* sp. (Fig. 7a), plates of echinoderms, corals, bryozoa, fragments of mollusks and brachiopods, orbitoids, alga, and globigerinids.

#### 5.1.4 | Raw geomaterials associated with Eocene basalts

Yellow and red Fe-based geomaterials are associated with Eocene Basalts at *San Giovanni Ilarione* (SGI) and *Località Salgari* (LS). Red geomaterials (samples SGI and LS) are homogeneous and isotropic. Rounded grains of basaltic rocks (grain size 0.8 mm) contain elongate plagioclase crystals in a vitreous matrix with an intersertal texture; volcanic glass, exhibiting ellipsoidal vesicles that are partially or completely replaced by Fe-rich material are remnants of the pyroclastic activity. Opaque minerals are widespread within the red matrix; accessory minerals are hematite, angular fragments of detrital quartz both as individual crystals 0.4 mm in diameter and as polycrystalline aggregates 0.8 mm in diameter. The matrix is composed of kaolinite and montmorillonite, while the opaque minerals correspond to anatase; the orange-red color is due to the presence of hematite and goethite as accessory phases (Cavallo, Riccardi et al., 2015). The composition is very similar to that reported in Cavallo and Zorzin (2014) for samples collected from the same area.

Yellow-brown geomaterials (samples SGI) are homogeneous and isotropic. Opaque minerals are widespread within the matrix; angular quartz 10 $\mu$m in diameter, pyroxenes and fragments of volcanic glass are present in small quantities. The matrix is composed of kaolinite and montmorillonite, while the opaque minerals correspond to anatase; the color is due to the presence of goethite.

#### 5.1.5 | Raw geomaterials associated with Eocene volcanoclastic terrains and Eocene limestones

The *Buso del Fero* (BF) mine has been operating since the 15th century (Longhi, 1979) for the exploitation of goethite and pyrolusite. It was included in this study as Fe-based geomaterials are found at the junction of Eocene volcanoclastic terrains and Eocene limestones. Representative samples were collected and goethite can be found in different mineral paragenesis. Goethite is associated with (1) clay minerals, (2) large crystals of secondary calcite, (3) nodules in the Eocene limestones and as incrustation of fossils, and (4) volcanic glass and its alteration products.

### 5.2 | Archaeological ocher

#### 5.2.1 | Fumane cave

Samples from Units A and D (Table II; A1-72b, A1-72h, A2-96-97, A2-46g, A1+A2-97, A2R-126g(1), D6-125c, D3d-68a, D3d-68b) exhibit dolomite crystals that are generally subhedral, sometimes zoned and turbid due to the presence of ferruginous compounds (ferroan dolomite or ankerite); the average size of the dolomite crystals is 50 $\mu$m in diameter. An Fe-based reddish coating with Ca-carbonates (secondary calcite) and Ca-phosphates (apatite) evenly covers the entire surface of each fragment. The fragments A2-110d and A2R-126g(2) are flat and very large showing an irregular pinkish layer that is 50–100 $\mu$m thick, coating the surface in an uneven manner. In addition, the fragments exhibit the presence of ooids cemented with a mosaic of partially dolomitized sparry calcite (euhedral dolomite crystals 100–200 $\mu$m across) with a texture similar to that of the cave bedrock. The mineralogical composition of these fragments (reported as Type 1 in Table IV) indicates that they can be tied to the Mesozoic dolomitized limestones. Markedly different is the fragment D3-137d(R) (Type 2, Table IV) composed of quartz and Fe-oxides. Electron microscopic analysis made it possible to detect that the quartz crystals are not homogeneous, contacts are indistinct, and that intracrystalline discontinuities occur. In addition, intracrystalline Fe-oxide concentrates in rounded isolated structures or as intercrystalline agglomerate particles. The remaining yellow fragments (Type 3 in Table IV, specifically A1-72g, A2-77c, A2-90e, D3-137d) are isotropic under the optical microscope. Finally, samples A2R-147h (red) and A2R-147h (yellow) (Type 4 in Table IV) are noteworthy since they are, respectively, composed of Fe-oxides and/or Fe-oxyhydroxides exhibiting a significant amount of bone fragments (Ca-phosphate).

#### 5.2.2 | Tagliente Rockshelter

On the basis of the petrographic analysis conducted on yellow and red ocher samples of the interior and exterior occupation areas of the site supported by XRPD (Cavallo, Fontana et al., 2015), a representative selection was made as reported in Table III. The primary group is composed of quartz + goethite and quartz + hematite (Type 2 in Table V), corresponding, respectively, to ~28% and ~17% of the total number of analyzed samples. These archaeological ocher samples generally exhibit a laminar microstructure due to the alternation of yellow and brown microlaminae, and have variable thickness (10–50 $\mu$m; occasionally up to 100 $\mu$m) distributed along parallel planes; in other cases this pattern is not marked, the microstructure is homogeneous and goethite mineral association exhibits acicular (50–100 $\mu$m long) and pseudohexagonal shapes (15–30 $\mu$m in diameter). Quartz exhibits anomalous interference colors due to the presence of goethite except where it occurs as individual mineral phase. The samples where quartz is associated with hematite show the same textural characteristics. Quartz crystals do not show distinct boundaries, inter- and intracrystalline microcracks occur probably indicating the attack of aggressive solutions. In addition, the morphologies connected with biomineralization processes were identified for the quartz-rich hematite ocher

**TABLE IV** Fumane Cave ocher typology

| Macrounit | Context | Square | Ocher Typology | Description |
|---|---|---|---|---|
| A | A1 | 72b | Type 1 | Dolomite-rich fragments (Mesozoic dolomitized limestones) |
| | A1 | 72h | | |
| | A2 | 96-97 | | |
| | A2 | 46g | | |
| | A2 | 110d | | |
| | A1 + A2 | 97 | | |
| | A2R | 126g(1) | | |
| | A2R | 126g(2) | | |
| D | D6 | 125c | | |
| | D3d | 68a | | |
| | D3d | 68b | | |
| D | D3 | 137d(R) | Type 2A | Quartz-rich hematite[a] (*Ponte di Veja*) |
| A | A1 | 72g | Type 3 | Goethite |
| | A2 | 90e | | |
| | A2 | 77c | | |
| D | D3 | 137d | | |
| A | A2R | 147h(R) | Type 4 | Hematite and goethite mixed with bone fragments |
| | A2R | 147h(Y) | | |

[a]After goethite thermal treatment.

samples. Seeing as the mineralogy and microstructure of the quartz-rich hematite is comparable with that of the quartz-rich goethite (both from archaeological and geological sources), it is possible to infer that the quartz-rich goethite was subjected to heat treatment (Fig. 8). The possibility of this type of processing has been already demonstrated for some archaeological ocher samples in previous research (Cavallo, Fontana et al., 2015) and through transmission electron microscopy (results not reported here).

The secondary group (Type 5 in Table Vb) is composed of quartz + calcite + hematite (12–8, 13–8) and quartz + calcite + goethite (418–50/1, 365–79/2, 12–25, 363–82/6_Ya, 363–82/6_Yb), corresponding, respectively, to approximately 7% and 9% of the total number of the analyzed samples. They demonstrate a laminar microstructure where quartz-rich laminae alternate with goethite or hematite-rich laminae with the presence of subangular crystals of sparry calcite exhibiting a low-medium sphericity.

The final group (Type 1 in Table V) is composed of the mineralogical association ankerite/dolomite + hematite and ankerite + calcite + hematite, corresponding, respectively, to 4% and 8% of the total number of the analyzed samples. Dolomite (ferroan) is generally anhedral, and the crystal size variability is generally unimodal (30–50 $\mu$m across) with the exception of large euhedral crystals 100–200 $\mu$m across (samples 15–22, 16–22, 361–53/1, 11A 35/8–34/2); ankerite occurs as euhedral zoned crystals with Fe-oxides concentrated along the rhombohedral cleavage (sample 361–53/1) and in the form of drusy spar (sample 358–69/3). Intercrystalline areas of dolomite are filled with hematite. Sparry calcite occurs in the majority of the analyzed samples. The petrographic observations of this set of samples indicate that they have a common origin tied to the Mesozoic dolomitized limestones.

## 6 | DISCUSSION

The microscopic investigations (PLM and SEM/EDXS) conducted on the archaeological ocher fragments excavated at Fumane Cave and Tagliente Rockshelter were compared with those from potential geological sources. The *Buso del Fero* mine (BF) must be excluded as potential source for several reasons. First, it was used in historical times (the mine was included in this study in order to have a complete view of the Fe-based deposits in the studied area). Second, archaeological ocher fragments never contain fragments or traces of volcanic glass that is a constituent of the Eocene volcanoclastites. Third, XRPD (Cavallo, Fontana et al., 2015) allowed for the detection of clay minerals (montmorillonite) that were never found in the analyzed archaeological ocher samples. For similar reasons, the composition of the yellow and red raw materials originating from the weathering of Eocene basalts located in *San Giovanni Ilarione* (SGI and LS samples) never correspond to the archaeological ocher in terms of mineralogical composition or texture and microstructure. This deposit—if we exclude the limited pocket at the mine of *Sant'Andrea* (SA), the *Cà Vecchi* Mine not reported in this research as it is only recently discovered, and the red laminae in the "shark" gallery at *via Tirapelle* (VTs)—is the most important outcrop of natural red Fe-based geomaterials in the area. This fact, combined with the extensive presence of red archaeological ocher, represents indirect evidence that the heating of yellow ocher was a common practice in the area as already demonstrated in other nearby archaeological contexts (Gialanella et al., 2011), and for some selected samples in Tagliente Rockshelter through the use of XRPD (Cavallo, Fontana et al., 2015).

None of the archaeological ocher samples exhibit sequences of layers of variable thickness, color, and composition as those found in the

**TABLE V** Tagliente rockshelter ocher typology: (a) interior and (b) exterior series

| (a) | | | | |
|---|---|---|---|---|
| **Macrounit** | **Context** | **Square** | **Ocher Typology** | **Description** |
| 1st | 302 | 55/8 | Type 2 | Quartz-rich goethite/hematite[a] (*Ponte di Veja*) |
| 2nd | 359 | 69/2 | | |
| 3rd | 358 | 69/3 | Type 1 | Dolomite-rich fragments (Mesozoic dolomitized limestones) |
| | 13A$\alpha$ | 85/6 | Type 2A | Quartz-rich hematite[a] (*Ponte di Veja*) |
| | 13 | 39/2 | Type 1 | Dolomite-rich fragments (Mesozoic dolomitized limestones) |
| | 13$\alpha$ | 42/3 | | |
| | 13 | 69/6 | | |
| T12 | 12 | 54/1,2,3 | | |
| **(b)** | | | | |
| T4 | 4(b) | 22 | Type 2 | Quartz-rich goethite/hematite[a] (*Ponte di Veja*) |
| T5 | 5 | 22 | | |
| T6 | 6 | 6 | | |
| | 6 | 6 | | |
| T7 | 7 | 80/7 | | |
| T8 | 8 | 20/2 | | |
| | 8 | 51/6 | | |
| T9 | 9 | 23 | | |
| T10 | 10a | 80/4 | | |
| | 10a | 80/4 | | |
| | *10b* | *80/7* | | |
| | 10c | 8 | | |
| | 10d | 64/8 | | |
| | 10f | 37 | | |
| T11 | 11A | 35/8–34/2 | Type 1 | Dolomite-rich fragments (Mesozoic dolomitized limestones) |
| | 361 | 53/1 | | |
| T12 | 363 | 82/6 | Type 5 | Quartz + calcite + goethite/hematite[a] (*Ponte di Veja*) |
| | 363 | 82/6 | | |
| | 12 | 8 | | |
| | 12 | 25 | | |
| T13 | 13 | 8 | | |
| T13–T14 | 365 | 79/2 | | |
| | 418 | 50/1 | | |
| T15 | 15 | 22 | Type 1 | Dolomite-rich fragments (Mesozoic dolomitized limestones) |
| T16 | 16 | 22 | | |

[a]After goethite thermal treatment.
10b-80/7 = Type 5.

deposits filling paleokarst caves associated with the Eocene limestones (VT and CO). Characteristic minerals for the Fe-based geomaterials associated with the Eocene limestones include glauconitic minerals, euhedral–subhedral dolomite crystals 50 $\mu$m in diameter, kaolinite, detrital fractions composed of muscovite, biotite, and quartz, as well as characteristic bioclasts. The only two archaeological fragments consisting of these distinctive minerals (muscovite and glauconitic minerals) are from Tagliente Rockshelter (ID 358–69/1, 3rd phase, internal area; T13–14 365–21/7,4,1 as in Cavallo, Fontana et al., 2015). All the remaining samples, including those from Fumane Cave, do not have characteristics that correspond to those of the Eocene limestones.

Most of the samples from Tagliente Rockshelter have a texture, microstructure, and composition related to the quartz-rich goethite

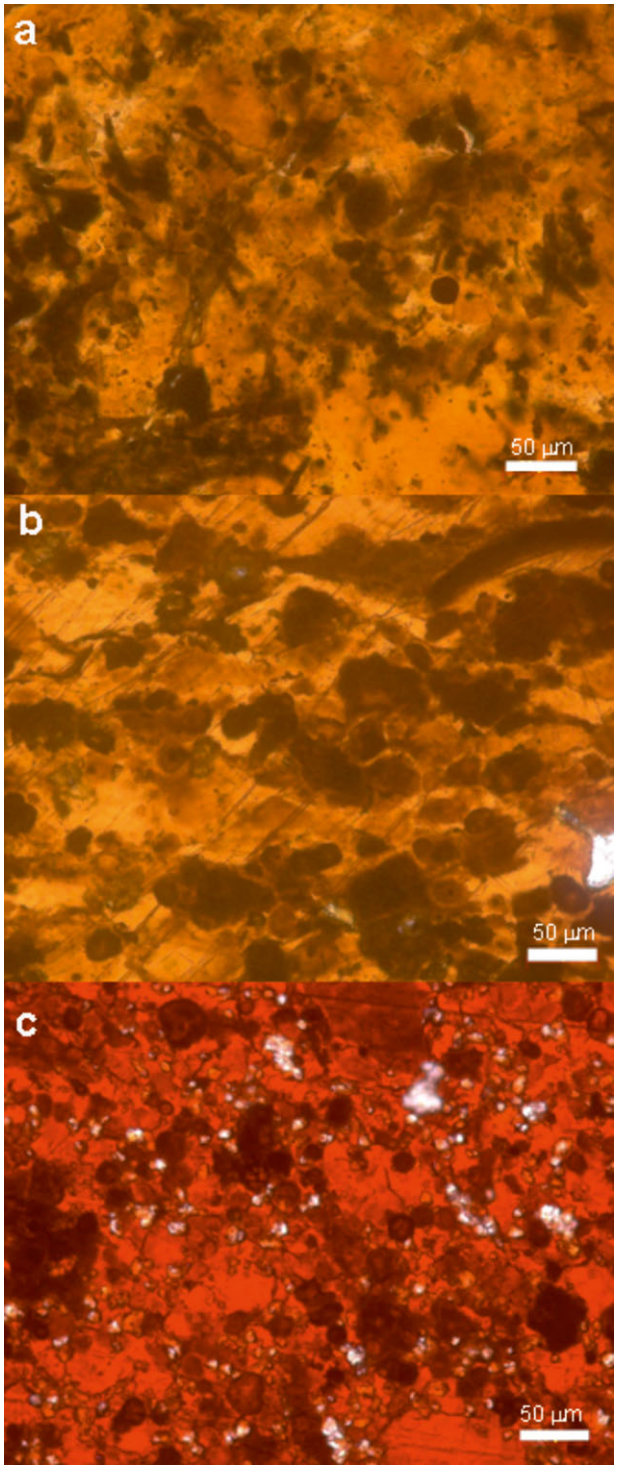


**FIGURE 8** Comparison of characteristic quartz-rich textures; (a) quartz-rich goethite from *Ponte di Veja*, Cave G; (b) quartz-rich goethite from Tagliente Rockshelter; (c) quartz-rich hematite from Tagliente Rockshelter (all micrographs under PLM, PPL; all images width = 0.45 mm) [Color figure can be viewed at wileyonlinelibrary.com]

that can be found at *Ponte di Veja* in caves G and D = E. The *Ponte di Veja* caves are the only potential source in the area where this type of material occurs. The similarity of the microstructure of quartz-rich goethite and quartz-rich hematite, and the complete absence of quartz-rich hematite deposits within the investigated geographical area can be interpreted as evidence of the thermal treatment of quartz-rich goethite fragments as already reported in Cavallo, Fontana et al. (2015). Only one of the analyzed red samples at Fumane Cave matches the site at *Ponte di Veja* (sample D3-137d-R); however the possibility that this sample underwent a heat treatment should be considered as well.

Many samples of dolomite from Fumane Cave reflect the composition of the Mesozoic dolomitized limestones. A few hypotheses can be proposed to explain this fact. The first hypothesis is that they correspond to rock fragments that have fallen down from the interior walls of the cave, and the red color on the surface can be interpreted as a ferruginous patina or a postdepositional event. Some rock flakes that are certainly related to detachments show the typical composition and texture of the (partially) dolomitized oolitic limestones that is different from that which was identified in the remaining dolomite-rich fragments. The second hypothesis is that these fragments come from the (fully) dolomitized oolitic limestone outcropping at *Manune* whose texture, microstructure, and composition closely match that of the archaeological samples. It is very difficult to determine whether these fragments were introduced into the archaeological site intentionally or transported there through geological processes. It is important to note that similar petrographic characteristics are shared with the geomaterials from *Sant'Andrea* and *San Bortolo*.

The petrographic examination of selected yellow and red ocher samples from Tagliente Rockshelter allowed for the identification of the sourcing area for the most important group of samples. Through comparing the textural, microstructural, and compositional results, it was possible to conclude that the only instance where goethite is associated with quartz featuring characteristic microlaminar structure indicative of biomineralization processes is in the samples coming from the caves D = E and G at *Ponte di Veja* (PV). In addition, many quartz-rich hematite archaeological ocher samples have the same characteristics of quartz-rich goethite samples that do not have any evidence within the study area. This fact, combined with evidence gathered from previous research (Cavallo, Fontana et al., 2015), supports the hypothesis that the quartz-based goethite was subjected to a heat treatment and will be further discussed in future papers. Only one sample from Fumane Cave can be attributed to this ocher type (Type 2 in Tables IV and Va and b).

The second important group found at Tagliente Rockshelter (Type 5 in Table Vb) where calcite is present as an accompanying mineral with quartz and goethite or hematite can be tied to the same geological sourcing area (*Ponte di Veja*). No samples with these characteristics were found at Fumane Cave and in the interior series at Tagliente Rockshelter in the analyzed samples.

Finally, the carbonate-based red ocher fragments found at both sites, but more extensively at Fumane Cave (Type 1 in Tables IV and Va and b), can be easily related to the weathering of Mesozoic dolomitized limestones that occur with similar characteristics at the *Manune* (MA), *Sant'Andrea* (SA), and *San Bortolo* (SB) sites, although the presence of red material is quite scarce.

On the basis of microscopic observations, it was not possible to understand the origin of ocher Types 3 and 4 through characteristic

minerals association or by studying textural and microstructural features.

The petrographic examination of the selected ocher materials reported in this research allowed possible procurement strategies to be highlighted. The most prevalent geological raw material found at Fumane Cave is dolomite-based with the exception of one quartz-rich sample (Table IV). Some of these samples are clearly related to the flaking of the cave vault and others can be tied to dolomitized limestones that outcrop extensively both close to the cave (*Manune*) and at a distance of about 20 km away (*Sant'Andrea* and *San Bortolo*).

The principal material found at Tagliente Rockshelter (Table Va and b) is quartz-based goethite (and hematite), which can be found only in the caves G and D = E at *Ponte di Veja* at a distance of about 8 km from the archaeological site. In addition, the material reported as Type 5 in Table Vb (quartz + calcite + goethite/hematite) comes from the same geological site and was found exclusively in the exterior series. Finally, the dolomite-based ocher has similar characteristics to those discussed for Fumane Cave.

If it is assumed that the geological resources that we find today are as those available during the prehistoric period, the following considerations arise. The inhabitants who lived at Fumane Cave preferred carbonate-based resources during the different stages of occupation of the site (macrounits A and D). However at Tagliente Rockshelter, procurement strategies can be further understood as quartz-based ocher prevails in the oldest microunits (first and second for the interior series; T4–T10 for the exterior series), while carbonate-based resources (dolomite and calcite with detrital quartz) prevail for the macrounits corresponding to the more recent occupation levels of the site (third and fourth for the interior series with the exception of the context 13A$\alpha$; T11–T16). Based on this evidence, there was a clear change in the procurement strategies practiced by the inhabitants of this site. It is very difficult to explain the reasons for this change due to the absence of information from other sites in the same region and the absence of wear traces on most of the samples. It is also apparent that Fe-based geomaterials are located within a "home range" area that would allow for a round trip within a day (Pradeau et al., 2016 and references therein).

Most of the artifacts are fragments of the original blocks. In Fumane Cave there is direct evidence of the ocher used as pigment. The raw material was powdered, and most probably intentionally mixed with bone fragments in order to obtain a painting material; evidence of the deliberate mixing of ocher and bone can also be found in South Africa at Blombos Cave where a tool kit (shell) containing ocher powder, bone fragments, and charcoal was found (Henshilwood et al., 2011).

## 7 | CONCLUSIONS

The analysis of the texture, microstructure, and composition of the accompanying minerals present in goethite- and hematite-based archaeological ocher and of potential geological sources for the raw materials demonstrates a valid approach in provenance studies. In the case of Fumane Cave, fragments of (ferroan) dolomite associated with hematite are sourced from the Mesozoic dolomitized limestones that outcrop at *Manune* close to the cave and *Sant'Andrea* (and *San Bortolo*) mines. The sourcing area for the remaining goethite or hematite samples—lacking in any accompanying minerals—cannot be identified. Only one sample can be connected to *Ponte di Veja* even if the hypothesis relating to heat treatment is correct. The remaining samples have texture, microstructure, and composition that closely resemble that of the cave bedrock.

As regards to Tagliente Rockshelter, the sourcing areas have been identified for two-thirds of the bulk of analyzed samples. These correspond to *Ponte di Veja* (yellow and red ocher) and the Mesozoic dolomitized limestones that outcrop at *Manune* and *Sant'Andrea* (red ocher samples), *San Bortolo* (for this site the possibility of heat treatment should be considered).

Based on this evidence, it is rather clear that during the relevant time period, the procurement areas for yellow and red ocher were local and that most of the materials analyzed are quartz-based geomaterials. Based on ocher typology distribution, it was possible to recognize deliberate strategies used in ocher procurement at Tagliente Rockshelter, while at Fumane Cave the collected materials remained quite the same during the different occupation phases of the site.

This research has raised many archaeological questions such as intentional selection of appropriate raw materials, technological processing, and final manipulation all linked to the use of ocher, particularly at Tagliente Rockshelter where there is no direct evidence concerning how the ocher was used. In addition, studies based on inductively coupled plasma mass spectrometry and quantitative textural analyses are planned for the future that will hopefully confirm and expand upon the results presented here.

## ACKNOWLEDGMENTS

We are very grateful to the anonymous reviewers whose comments, suggestions, and advice helped to improve the manuscript. We thank Professor Miriam Cobianchi of the University of Pavia for her palaeontological support and Elisabeth Manship for the final editing of the English text.

## REFERENCES

Arzarello, M., Bertola, S., Fontana, F., Guerreschi, A., Thun Hohenstein, U., Liagre, J., … Rocci Ris, A. (2007). Aires d'approvisionnement en matières premières lithiques et en ressources alimentaires dans les niveaux mousteriens et épigravettiens de l'Abri Tagliente (Verone, Italie): une dimension "locale" In M. H. Moncel, A.-M. Moigne, M. Arzarello, & C. Peretto (Eds.), *Aires d'approvisionnement en matières premières et aires d'approvisionnement en ressources alimentaires.* Approche intégrées des comportements, Proceedings of the XV U.I.S.P.P. Congress, Lisbona, 3-9 settembre 2006, B.A.R. International Series, *1725*, 161–169.

Arzarello, M., & Peretto, C. (2005). Données nouvelles sur les caractéristiques et l'évolution tecno-économique de l'industrie moustérienne du Riparo Tagliente (Verone, Italie). Colloque International: données récentes sur les modalités de peuplement et sur le cadre chronostratigraphique, géologique et paléogéographique des industries du

Paléolithique inférieur et moyen en Europe BAR International Series S1364, 281–289.

Bartolomei, G., Broglio, A., Cassoli, P., Castelletti, L., Cremaschi, M., Giacobini, G., … Tagliacozzo, A. (1992). La Grotte-Abri de Fumane. Un site Aurignacien au Sud des Alps. *Preistoria Alpina*, *28*, 131–179.

Bartolomei, G., Broglio, A., Cattani, L., Cremaschi, M., Guerreschi, A., Leonardi, P., & Peretto, C. (1984). Paleolitico e Mesolitico. In A. Aspes (Eds.), *Il Veneto nell'antichità. Preistoria e Protostoria* (Vol. *2*, pp. 167–319). Verona: Banca Popolare di Verona.

Bartolomei, G., Broglio, A., Cattani, L., Cremaschi, M., Guerreschi, A., Mantovani, E., … Sala, B. (1982). I depositi würmiani del Riparo Tagliente. Annali dell'Università di Ferrara. *Nuova serie, Sez. 15*, *3*(4), 51–105.

Bartolomei, G., Broglio, A., Guerreschi, A., Leonardi, P., Peretto, C., & Sala, B. (1974). Una sepoltura epigravettiana nel deposito pleistocenico del Riparo Tagliente in Valpantena (Verona). *Rivista di Scienze Preistoriche*, *29*(2), 1–52.

Bertola, S., Broglio, A., Cassoli, P., Cilli, C., Dalmeri, G., De Stefani, M., … Ziggiotti, S. (2007). L'Epigravettiano recente nell'area prealpina e alpina orientale. In F. Martini (Eds.), L'Italia tra 15.000 e 10.000 anni fa. Cosmopolitismo e regionalità nel Tardoglaciale. Atti della tavola Rotonda (Firenze 18 novembre 2005). Museo Fiorentino di Preistoria "Paolo Graziosi", Firenze 2007, Millenni, Studi di Archeologia Preistorica, 5, pp. 39–94.

Bietti, A., Boschian, G., Crisci, M. G., Danese, E., De Francesco, A. M., Dini, M., … Tykot, R. (2004). Inorganic raw materials economy and provenance of chipped industry in some stone age sites of Northern and Central Italy. *Collegium Anthropologicum, Zagreb (Croatia)*, *28*(1), 41–54.

Broglio, A., & Dalmeri, G. (2005). Pitture paleolitiche nelle Prealpi Venete: Grotta di Fumane e Riparo Dalmeri. *Memorie Museo Civico di Storia Naturale di Verona*, *9*, pp. 190.

Broglio, A., & Gurioli, F. (2004). Le comportement symbolique des premiers Hommes modernes: les données de la Grotte de Fumane (Pré-Alpes vénitiennes). In M. Otte (Ed.), La Spiritualité. ERAUL 106, 97–102.

Cavallo, G., Fontana, F., Gonzato, F., Guerreschi, A., Riccardi, M. P., Sardelli, G., &Zorzin, R. (2015). Sourcing and processing of ochre during the late upper Palaeolithic at Tagliente Rock-shelter (NE Italy) based on conventional X-ray powder diffraction analysis. *Journal of Archaeological and Anthropological Sciences*, *2015*. doi:10.1007/s12520-015-0299-3

Cavallo, G., Riccardi, M. P., & Zorzin, R. (2015). Powder diffraction of yellow and red natural earths from Lessini Mountains in NE Italy. *Powder Diffraction Journal*, *30*(2), 122–129.

Cavallo, G., Riccardi, M. P., & Zorzin, R. (2016). Natural yellow and red Fe-based geomaterials from the Lessini Mountains in Veneto, Italy: A review. *Color research and Application*. doi:10.1002/col.22039

Cavallo, G., & Zorzin, R. (2008). Preliminary data on the yellow ochre at the mine of *Via Tirapelle* in Verona (Italy). *X-Ray Spectrometry*, *37*:395–398.

Cavallo, G., & Zorzin, R. (2014). Geology, petrography, mineralogy, geochemistry of natural Fe-based pigments from Verona province (Italy). In R. B. Scott, D. Braekmans, M. Carremans, & P. Degryse (Eds.), Proceeding of the 39th International Symposium on Archaeometry. Center for Archaeological Sciences, KU Leuven, Belgium, 9–15.

Chalmin, E., Menu, M., & Vignaud, C. (2003). Analysis of rock-art painting and technology of Palaeolithic painters. *Measurement Science and Technology*, *14*, 1590–1597.

Cilli, C., Giacobini, G., Guerreschi, A., & Gurioli, F. (2006). L'industria e gli oggetti ornamentali in materia dura animale dell'epigravettiano di Riparo Tagliente (Verona). Atti della XXXIX Riunione Scientifica "Materie prime e scambi nella preistoria italiana," Firenze, 25–27 novembre 2004, vol. II, 843–854.

Cilli, C., & Guerreschi, A. (2000). Studio archeozoologico e tafonomico di un'area di concentrazione di reperti faunistici di età epigravettiana (Riparo Tagliente, Verona). Atti del 2° Convegno Nazionale di Archeozoologia, Asti, 1997. ABACO Ed., Forli, 141–149.

Cremona, M. G., & Fontana, F. (2007). Analisi tecno-economica di una concentrazione di scarti litici (US 411) dai livelli epigravettiani di Riparo Tagliente (Stallavena di Grezzana, Verona). Atti del Convegno Nazionale degli Studenti di Antropologia, Preistoria e Protostoria, Ferrara 8-10 Maggio 2004, Annali dell'Università degli Studi di Ferrara - Museologia Scientifica e Naturalistica, volume speciale 2007, 59–62.

Dayet, L., Texier, P.-J., Daniel, F., & Porraz, G. (2013). Ochre resources from the Middle Stone Age sequence of Diepkloof Rock Shelter, Western Cape, South Africa. *Journal of Archaeological Science*, *40*, 3492–3505.

Douka, K., Higham, T. F. G., Wood, R., Boscato, P., Gambassini, P., Karkanas, P., … Ronchitelli, A. (2014). On the chronology of the Uluzzian. *Journal of Human Evolution*, *68*, 1–13.

Eriarte, E., Foyo, A., Sánchez, M. A., Tomillo, C., & Setién, J. (2009). The origin and geochemical characterization of red ochre from the Tito Bustillo and Monte Castillo caves (Northern Spain). *Archaeometry*, *51*(2), 231–251.

Fiore, I., Gala, M., Romandini, M., Cocca, E., Tagliacozzo, A., & Peresani, M. (2016). From feathers to food: Reconstructing the complete exploitation of avifaunal resources by Neanderthals at Grotta di Fumane, Unit A9. In R. Blasco & M. Peresani (Eds.), *Hominid-bird interactions in prehistory*. Session B8, XVII UISPP Congress. Quaternary International, *421*, 134–153.

Fontana, F., Cilli, C., Cremona, M. G., Giacobini, G., Gurioli, F., Liagre, J., … Guerreschi, A. (2009). Recent data on the Late Epigravettian occupation at Riparo Tagliente, Monti Lessini (Grezzana, Verona): A multidisciplinary perspective. Proceedings of the 49th Hugo Obermeier Society Meeting, Trento, 10–14 Aprile 2007, Preistoria Alpina, *44*, 51–59.

Fontana, F., Cremona, M., Falceri, L., Gajardo, A., Ndiaye, M., Neri, A., … Guerreschi, A. (2012). Lithic technical systems in the first part of the late glacial at Riparo Tagliente (Stallavena Di Grezzana, Verona). In XIX Congresso dell'Associazione Antropologica Italiana. 1961-2011: cinquant'anni di congressi. Passato, presente e futuro dell'antropologia. Torino, 21-24 settembre 2011, Journal of Biological Research, LXXXIV (2011), *1*, 102–103.

Fontana, F., Guerreschi, A., Bertola, S., Bonci, F., Cilli, C., Liagre, J., … Thun Hohenstein, U. (2008). The first occupation of the Southern Alps in the Late Glacial at Riparo Tagliente (Verona, Italy). Detecting the organisation of living-floors through a G.I.S. integrated analysis of technological, functional, palaeoeconomic and spatial attributes. In S. Grimaldi & T. Perrin (Eds.), *Mountain environments in prehistoric Europe: Settlement and mobility strategies from Palaeolithic to the early Bronze age*. Proceedings of the XV U.I.S.P.P. Congress, Lisbona, 3-9 settembre 2006, Session C31, (Series Editor L. Oosterbeek), B.A.R. international series. Vol. 26, Oxford: Archaeopress, 71–79.

Fontana, F., Guerreschi, A., Bertola, S., Cremona, M. G., Cavulli, F., Falceri, L., … Visentin, D. (2015). I livelli più antichi della serie epigravettiana "interna" di Riparo Tagliente: sfruttamento delle risorse litiche e sistemi tecnici. In G. Leonardi & V. Tinè (Eds.), Atti della XLVIII Riunione Scientifica dell'Istituto Italiano di Preistoria e Protostoria, Preistoria e Protostoria del Veneto, Padova 5-9 novembre 2013, Istituto Italiano di Preistoria e Protostoria, 43–52.

Fontana, F., Guerreschi, A., & Liagre, J., (2002). Riparo Tagliente. La serie epigravettiana. In A. Aspes (Ed.), *Preistoria Veronese. Contributi e aggiornamenti*, *Memorie del Museo Civico di Storia Naturale di Verona*, *2nd series*, Scienze dell'Uomo, *5*, pp. 42–47.

Forte, M. (2016). L'importanza dell'Archeomalacologia negli studi archeologici. Analisi della collezione malacologica marina aurignaziana della

Grotta di Fumane come esempio di caso-studio (Unpublished MA thesis). University of Ferrara, Italy.

Gazzoni, V., Goude, G., Herrscher, E., Guerreschi, A., Antonioli, F., & Fontana, F. (2013). Late upper Palaeolithic human diet: First stable isotope evidence from Riparo Tagliente (Verona, Italy). *Bulletin et mémoires de la Société d'Anthropologie de Paris*, *25*(1), 103–117.

Gialanella, S., Belli, R., Dalmeri, G., Lonardelli, I., Mattarelli, M., Montagna, M., & Toniutti, L. (2011). Artificial or natural origin of hematite-based red pigments in archaeological contexts: The case of Riparo Dalmeri (Trento, Italy). *Archaeometry*, *53*(5), 950–962.

Gonzato, G., Castellarin, A., Chignola, R., Gamberini, F., Lazzeri, P., & Unione Speleologica Veronese (2014). New dating of palaeokarst features at Torricelle hills (Verona, Italy). *Italian Journal of Geoscience*, *133*(3), 427–438.

Green, R. L., & Watling, R. J. (2007). Trace element fingerprinting of Australian ochre using laser ablation inductively coupled plasma-mass spectrometry (LAICP-MS) for the provenance establishment and authentication of indigenous art. *Journal of Forensic Science*, *52*(4), 851–859.

Guerreschi, A. (1983). Structures d'habitat épigravettiennes dans l'Abri Tagliente (Verone) et dans la grotte du Prete (Ancone-Italie). In H. Berke, J. Hahn, & C. J. Kind (Eds.), Proceedings of the International conference "Upper Paleolithic settlement patterns in Europe," *Archaeologica Venatoria. Vol. 6*, Gunzburg: Reisensburg, 59–67.

Guerreschi, A., & Veronese, C. (2002). L'Epigravettiano di Riparo Tagliente: evidenze archeologiche di comportamenti simbolici. In: A. Aspes (Eds.) *Preistoria Veronese. Contributi e aggiornamenti*, *Memorie del Museo Civico di Storia Naturale di Verona*, *2^ serie*, *sez*. Scienze dell'Uomo, *5*, 42–47.

Henshilwood, C. S., d'Errico, F., van Niekerk, K. L., Coquinot, Y., Jacobs, Z., Luritzen, S.-E., … García-Moreno, R. (2011). A 100,000-year-old ochre-processing workshop at Blombos Cave, South Africa. *Science*, *334*, 219–222. doi:10.1126/science.1211535

Higham, T., Brock, F., Peresani, M., Broglio, A., Wood, R., & Douka, K. (2009). Problems with radiocarbon dating the Middle and Upper Palaeolithic transition in Italy. *Quaternary Science Review*, *28*, 1257–1267.

Hodgskiss, T. (2010). Identifying grinding, scoring and rubbing use-wear on experimental ochre pieces. *Journal of Archaeological Science*, *37*, 3344–3358.

Longhi, A. 1979, *Miniere e minerali del veronese. Ed*. Verona: Libreria Cortina.

MacDonald, B. L., Hancock, R. G. V., Cannon, A., McNeill, F., Reimer, R., & Pidruczny, A. (2013). Elemental analysis of ochre outcrops in the southern British Columbia, Canada. *Archaeometry*, *55*(6), 1020–1033.

MacDonald, B. L., Hancock, R. G. V., Cannon, A., & Pidruczny, A. (2011). Geochemical characterization of ochre from central coastal British Columbia, Canada. *Journal of Archaeological Science*, *38*, 3620–3630.

Marmolejo-Rodríguez, A. J., Prego, R., Meyer-Willerer, A., Shumilin, E., & Sapozhnikov, D. (2007). Rare earth elements in iron oxy–hydroxide rich sediments from the Marabasco River-Estuary System Pacific coast of Mexico. REE affinity with iron and aluminium. *Journal of Geochemical Exploration*, *94*, 43–51.

Martini, M., Sibilia, M., Croci, S., & Cremaschi, M. (2001). Thermoluminescence (TL) dating of burnt flints: Problems, perspectives and some example of application. *Journal of Cultural Heritage*, *2*, 179–190.

Moreau, L., Brandl, M., Filzmoser, P., Hauzenberger, C., Goemaere, É., Jadin, I., … Schmitz, R. W. (2016). Geochemical sourcing of flint artifacts from western Belgium and the German Rhineland: Testing hypotheses on Gravettian period mobility and raw material economy. *Geoarchaeology*, *31*, 229–243.

Pallecchi, P. (2005). Caratterizzazione delle ocre rinvenute nella grotta e confronto con alcuni giacimenti di ocra gialla e rossa del veronese. In: A. Broglio & G. Dalmeri, *Pitture paleolitiche nelle Prealpi Venete: Grotta di Fumane e Riparo Dalmeri*. Memorie Museo Civico di Storia Naturale di Verona, *9*, 54–57.

Peresani, M. (2012). Fifty thousand years of flint knapping and tool shaping across the Mousterian and Uluzzian sequence of Fumane Cave. *Quaternary International*, *247*, 125–150.

Peresani, M., Chravzez, J., Danti, A., De March, M., Duches, R., Gurioli, F., … Trombino, L. (2011). Fire-places, frequentations and the environmental setting of the final Mousterian at Grotta di Fumane: A report from the 2006–2008 research. *Quartär*, *58*, 131–151.

Peresani, M., Cremaschi, M., Ferraro, F., Falguères, C., Bahain, J. J., Gruppioni, G., … Dolo, J. M. (2008). Age of the final Middle Palaeolithic and Uluzzian levels at Fumane Cave, Northern Italy, using 14C, ESR, 234U/230Th and thermoluminescence methods. *Journal of Archaeological Science*, *35*, 2986–2996.

Peresani, M., Cristiani, E., & Romandini, M. (2016). The Uluzzian technology of Grotta di Fumane and its implication for reconstructing cultural dynamics in the Middle—Upper Palaeolithic transition of Western Eurasia. *Journal of Human Evolution*, *91*, 36–56.

Peresani, M., Fiore, I., Gala, M., Romandini, M., & Tagliacozzo, A. (2011b). Late Neandertals and the intentional removal of feathers as evidenced from bird bone taphonomy at Fumane Cave 44 ky B.P., Italy. *Proceedings of the National Academy of Sciences*, *108*, 3888–3893.

Peretto, C., Biagi, P., Boschian, G., Broglio, A., de Stefani, M., Fasani, L., … Tozzi, C. (2004). Living-floors and structures from the lower Palaeolithic to the Bronze Age. *Collegium Antropologicum*, *28*(1), 63–88.

Popelka-Filcoff, R. S., Robertson, J. D., Glascock, M. D., & Descantes, C. (2007). Trace element characterization of ochre from geological sources. *Journal of Radioanalytical and Nuclear Chemistry*, *272*(1), 17–27.

Pradeau, J.-V., Binder, D., Vérati, C., Lardeaux, J.-M., Dubernet, S., Lefrais, Y., & Regert, M. (2016). Procurement strategies of Neolithic colouring materials: Territoriality and networks from 6th to 5th millennia BCE in North-Western Mediterranean. *Journal of Archaeological Science*, *71*, 10–23.

Rifkin, R. F. (2012). Processing ochre in the Middle Stone Age: Testing the inference of prehistoric behaviours from actualistically derived experimental data. *Journal of Anthropological Archaeology*, *31*, 174–195.

Rocci Ris, A., Cilli, C., Malerba, G., Giacobini, G., & Guerreschi, A. (2005). Archeozoologia e tafonomia dei reperti provenienti da un complesso epigravettiano (taglio 10) di Riparo Tagliente (Grezzana, VR). In: G. Malerba & P. Visentini (Eds.), *Atti del 4° Convegno nazionale di Archeozoologia AIAZ. (Pordenone, 13-15 novembre 2003)*. Quaderni del Museo Archeologico del Friuli Occidentale, *6*, 111–123.

Romandini M., Nannini N., Tagliacozzo A., & Peresani M. (2014). The ungulate assemblage from layer A9 at Grotta di Fumane, Italy: a zooarchaeological contribution to the reconstruction of Neanderthal ecology. *Quaternary International*, *337*, 11–27.

Thun Hohenstein, U., & Peretto, C. (2005). Faunal exploitation in the Middle Palaeolithic: Evidences from Riparo Tagliente (Verona, Italy). Actes du Colloque International: Donnees récentes sur les modalités de peuplement et sur le cadre chronostratigraphique, géologique et paléogéographique des industries du Paléolithique inférieur et moyen en Europe, Bar International Series 1364, Oxford. 261–267.

Wadley, L. (2010). Cemented ash as a receptacle or work surface for ochre powder production at Sibudu, South Africa, 58,000 years ago. *Journal of Archaeological Science*, *37*, 2397–2406.

Woodward, J. C., & Goldberg, P. (2001). The sedimentary records in Mediterranean rockshelters and caves: Archives of environmental change. *Geoarchaeology*, *16*(4), 327–354.

Woodward, J. C., Hamlin, R. H. B., Macklin, P., Karkanas, P., & Kotjabopoulou, E. (2001). Quantitative sourcing of slackwater deposits at Boila Rockshelter: A record of late glacial flooding and Palaeolithic settlement in the Pindus Mountains, Northwest Greece. *Geoarchaeology*, *16*(5), 501–536.

Zampieri, D., & Zorzin, R. (1993). L'assetto stratigrafico. In L. Sorbini (Ed.), *Geologia, Idrogeologia e Qualità dei principali acquiferi veronesi. Memorie del Museo Civico di Storia Naturale di Verona (IIa serie)*, Sezione Scienze della Terra, *4*, 23–26.

Zorzin, R. (1993). Analisi quantitativa della struttura e delle cavità carsiche. In L. Sorbini (Ed.), *Geologia, Idrogeologia e Qualità dei principali acquiferi veronesi. Memorie del Museo Civico di Storia Naturale di Verona (II serie)*, Sezione Scienze della Terra, *4*, 35–38.

Zorzin, R., & Stradiotto, G. (1995). Nuovi dati sul paleocarsismo delle Torricelle (Monti Lessini-Verona). *Speleologia Veneta*, *Nuova serie*, *3*, 51–59.

**How to cite this article:** Cavallo G, Fontana F, Gonzato F, et al. Textural, microstructural, and compositional characteristics of Fe-based geomaterials and Upper Palaeolithic ochre in the Lessini Mountains, Northeast Italy: Implications for provenance studies. *Geoarchaeology*. 2017;00:1–19. doi:10.1002/gea.21617